


RESEARCH ARTICLE

Differential YAP nuclear signaling in healthy and dystrophic skeletal muscle

Shama R. Iyer,¹ Sameer B. Shah,^{2,3} Christopher W. Ward,¹ Joseph P. Stains,¹ Espen E. Spangenburg,⁴ Eric S. Folker,⁵ and  Richard M. Lovering^{1,6}

¹Department of Orthopaedics, University of Maryland School of Medicine, Baltimore, Maryland; ²Department of Orthopaedic Surgery, University of California San Diego, La Jolla, California; ³Department of Bioengineering, University of California San Diego, La Jolla, California; ⁴Department of Physiology, East Carolina Diabetes and Obesity Institute, East Carolina University, Greenville, North Carolina; ⁵Department of Biology, Boston College, Chestnut Hill, Massachusetts; and ⁶Department of Physiology, University of Maryland School of Medicine, Baltimore, Maryland

Submitted 29 October 2018; accepted in final form 4 April 2019

Iyer SR, Shah SB, Ward CW, Stains JP, Spangenburg EE, Folker ES, Lovering RM. Differential YAP nuclear signaling in healthy and dystrophic skeletal muscle. *Am J Physiol Cell Physiol* 317: C48–C57, 2019. First published April 17, 2019; doi:10.1152/ajpcell.00432.2018.—Mechanical forces regulate muscle development, hypertrophy, and homeostasis. Force-transmitting structures allow mechanotransduction at the sarcolemma, cytoskeleton, and nuclear envelope. There is growing evidence that Yes-associated protein (YAP) serves as a nuclear relay of mechanical signals and can induce a range of downstream signaling cascades. Dystrophin is a sarcolemma-associated protein, and its absence underlies the pathology in Duchenne muscular dystrophy. We tested the hypothesis that the absence of dystrophin in muscle would result in reduced YAP signaling in response to loading. Following in vivo contractile loading in muscles of healthy (wild-type; WT) mice and mice lacking dystrophin (*mdx*), we performed Western blots of whole and fractionated muscle homogenates to examine the ratio of phospho (cytoplasmic) YAP to total YAP and nuclear YAP, respectively. We show that in vivo contractile loading induced a robust increase in YAP expression and its nuclear localization in WT muscles. Surprisingly, in *mdx* muscles, active YAP expression was constitutively elevated and unresponsive to load. Results from qRT-PCR analysis support the hyperactivation of YAP in vivo in *mdx* muscles, as evidenced by increased gene expression of YAP downstream targets. In vitro assays of isolated myofibers plated on substrates with high stiffness showed YAP nuclear labeling for both genotypes, indicating functional YAP signaling in *mdx* muscles. We conclude that while YAP signaling can occur in the absence of dystrophin, dystrophic muscles have altered mechanotransduction, whereby constitutively active YAP results in a failure to respond to load, which could be attributed to the increased state of “pre-stress” with increased cytoskeletal and extracellular matrix stiffness.

dystrophy; mechanotransduction; skeletal muscle

INTRODUCTION

Duchenne muscular dystrophy (DMD) is an X-linked myopathy characterized clinically by severe, progressive, and irreversible muscle wasting, and loss of muscular function (36). DMD is the most common and most severe form of muscular dystrophy and is caused by the lack of dystrophin, a large sarcolemma-associated protein expressed in striated mus-

cle. While the genetic basis for DMD has been determined, the mechanisms responsible for progressive muscle damage and weakness remain unclear. The *mdx* mouse, the most common animal model for DMD, also lacks dystrophin, resulting in deleterious effects on histopathology and function. The *mdx* muscle has significantly increased stiffness (2, 21, 32, 33) due to increased fibrosis (21) and increased expression of cytoskeleton components such as microtubules (4, 32, 33, 42) and desmin (4, 42). In addition, the absence of dystrophin results in altered nuclear-cytoskeletal coupling in skeletal muscle (26). The aim of this study was to provide further insight into aberrant nuclear mechanotransduction in dystrophic muscles, by characterizing the dynamic changes in the mechano-responsive factor Yes-associated protein (YAP) in response to loading in healthy and dystrophic muscles.

YAP is a transcriptional coactivator downstream of the Hippo pathway and has recently been found to play a key role in nuclear mechanotransduction in various tissues (1, 11, 12, 44), including skeletal muscle (14, 53). The highly conserved Hippo pathway regulates several cellular processes, including cell proliferation, apoptosis, various stress responses, and consists of a core kinase cascade (1, 11, 24, 31, 44, 55, 56). The name “Hippo” is derived from early work in *Drosophila*, whereby mutations in the gene locus led to tissue overgrowth, resulting in a hippopotamus-looking head (51). A canonical Hippo pathway has been described for mammals and intersects with diverse signaling pathways, including TGF- β , Wnt, and Akt-mammalian target of rapamycin pathways (15, 16).

In its activated state (i.e., nonphosphorylated), YAP translocates to the nucleus and regulates several transcription factors, resulting in modulation of a wide array of cellular functions. In skeletal muscle, YAP activity initiates diverse outcomes, including myogenesis and regeneration (12, 15, 16), as well as hypertrophy (18, 53). However, constitutively active YAP leads to muscle atrophy and degeneration (28). YAP levels decline during maturation of skeletal myofibers (53) and also after differentiation of satellite cells (29). YAP also regulates neuromuscular junction formation and regeneration in muscle (55) and regulates muscle fiber size to ameliorate neurogenic muscle atrophy (53). Despite ongoing work to clarify the Hippo pathway and its interaction with other signaling pathways, there is growing evidence that YAP nuclear translocation is a key indicator of mechanotransduction (11).

Address for reprint requests and other correspondence: R. Lovering, Univ. of Maryland School of Medicine, Dept. of Orthopaedics, AHB, Rm. 540, 100 Penn St., Baltimore, MD 21201 (e-mail: rlovering@som.umaryland.edu).

Nuclear translocation of YAP is seen with increases in substrate stiffness or mechanical stress in epithelial cells (1, 11), mesenchymal stem cells (10), osteoblasts (30, 31), fibroblasts (49), cardiac cells (40), and skeletal muscle precursor cells (myoblasts) (5). However, it remains unclear how mechanical stress promotes YAP nuclear translocation in mature skeletal muscle fibers. Studies have examined the effects of overexpressed or mutated YAP on muscle (28, 55), or changes in YAP expression in muscle with compensatory hypertrophy following synergistic ablation, wheel-running exercise following hindlimb suspension, or following myostatin/activin blockers (6, 18, 23). While YAP translocation to the nucleus in skeletal muscle has been reported after denervation and toxin injection (53), whether nuclear localization of YAP changes due to differences in substrate stiffness, or in response to physiological contractile loading, is less clear. Given the aberrant cytoskeletal and nuclear-cytoskeletal coupling, in addition to the increased stiffness in muscles lacking dystrophin, we speculated that YAP signaling is likely to be impaired in *mdx* muscle.

Thus we tested the hypothesis that the absence of dystrophin would result in reduced YAP signaling in response to loading.

To this end, we used perturbations including in vivo physiological muscle contractile loading and in vitro plating of fibers on substrates of varying stiffness. Surprisingly, while we found increased YAP signaling with loading in wild-type (WT) muscles, *mdx* muscles appeared constitutively active and not further increased by load. Furthermore, we found that *mdx* muscle fibers can become mechano-responsive, similar to WT muscle fibers, when plated on substrates of varying stiffness in vitro, suggesting that the pathway is operant but aspects of the in vivo environment in *mdx* mice impair normal YAP responsiveness.

MATERIALS AND METHODS

Animals. All protocols were approved by the University of Maryland Institutional Animal Care and Use Committee. All studies were conducted in compliance with the Animal Welfare Act, the Implementing Animal Welfare Regulations, and in accordance with the principles of the *Guide for the Care and Use of Laboratory Animals*. We used healthy (WT) mice and *mdx* (lacking dystrophin) mice from the C57BL/10ScSnJ strain (The Jackson Laboratory, Bar Harbor, ME). A total of 24 mice were used around at ~2–3 mo of age for both genotypes.

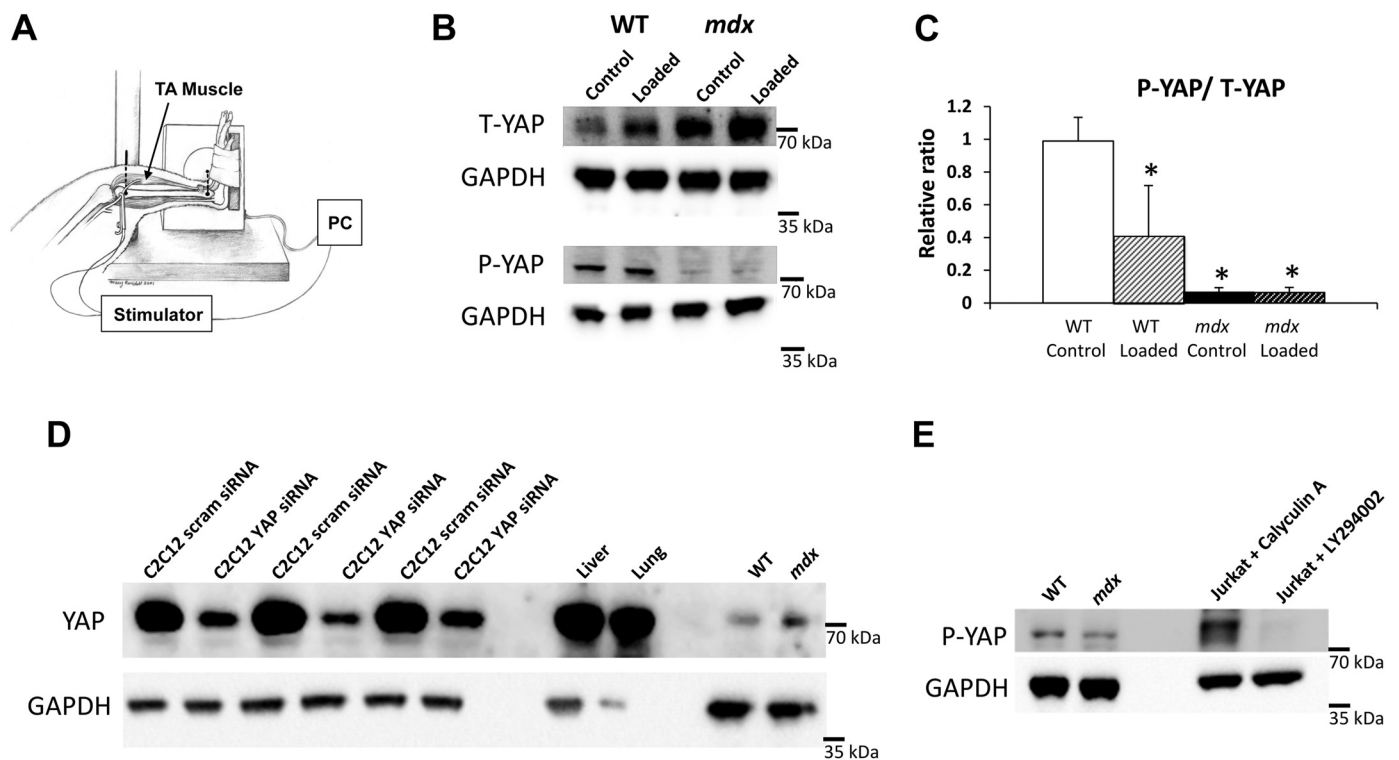


Fig. 1. Yes-associated protein (YAP) in *mdx* muscle is increased and unresponsive to in vivo loading. **A:** an established model was used to stabilize the hindlimb of an anesthetized mouse and subcutaneous electrodes at the fibular nerve to induce repeated maximal isometric contractions in the tibialis anterior (TA) muscle. **B:** phospho-YAP, total-YAP, and GAPDH protein expression in wild-type (WT) and *mdx* whole muscle homogenate with or without isometric loading. The cropped blots in each panel are from a single gel and single exposure of 4 contiguous lanes. Densitometry measures were normalized to GAPDH expression, and to respective control (no-load, contralateral) WT muscles. Values are means \pm SD for TA muscles from 4 animals per genotype and loading condition. **C:** relative phospho/total YAP ratio between WT and *mdx* muscles with or without loading relative to control WT muscles. Phospho/total YAP ratio is significantly different with loading in WT, but not in *mdx* muscles, indicative of impaired nuclear response to mechanical loading. However, phospho/total YAP ratio is significantly lower in *mdx* muscles with or without loading compared with control WT muscles. One-way ANOVA was performed on square-root-transformed data to determine statistical differences between groups. Antibody validation is also shown. * $P < 0.05$ compared with control WT. **D:** YAP and GAPDH protein expression in control C2C12 cells, C2C12 cells with siRNA-mediated YAP knockdown, liver and lung homogenates, and WT and *mdx* muscle homogenates. The controls in this case refer to C2C12 cells treated with scrambled si-RNA. **E:** P-YAP and GAPDH protein expression in WT and *mdx* muscle homogenates and Jurkat cells treated with calyculin A or LY294002. Calyculin A is a strong phosphatase inhibitor, while LY294002 is an inhibitor of phosphatidylinositol 3-kinase, with cells treated with LY294002 expressing low phospho-YAP expression. [Adapted from Lovering et al. (34a), with permission from Elsevier.]

In vivo contractile loading. Experimentation was performed with the animal anesthetized under 2–4% inhaled isoflurane. Body temperature was maintained by a heating lamp; thermal support was also supported by a thermostatically controlled warming pad (Deltaphase Isothermal Pad, Braintree Scientific). Maximal stimulation of the dorsiflexors in vivo was performed as described using an established model (27, 34, 37, 45). Briefly, with the animal placed in a supine position, the knee was stabilized and the foot was secured onto a foot plate (Fig. 1A). The axis of the ankle was aligned with the axis of the stepper motor (model T8904, NMB Technologies, Chatsworth, CA) and a torque sensor (QWFK-8M, Sensotec, Columbus, OH). The fibular nerve was stimulated via subcutaneous needle electrodes (J05 Needle Electrode Needles, 36BTP, Jari Electrode Supply, Gilroy, CA). Proper electrode position was determined by a series of isometric twitches and by observing isolated ankle dorsiflexion in the anesthetized animal. A custom program based on commercial software (LabView version 8.5, National Instruments, Austin, TX) was used to coordinate contractile maximal tetanic activation of 240 repetitions (300-ms train duration, 100 Hz) with a rest period of 30 s between contractions, to ensure no loss in force with fatigue. The unstimulated contralateral dorsiflexors served as controls. After the completion of the isometric loading regimen (~2 h in duration), the tissues were immediately harvested and snap frozen in liquid nitrogen.

Western blotting. Isometrically loaded and contralateral WT and *mdx* tibialis anterior (TA) muscles ($n = 4$ for WT, $n = 4$ for *mdx*) were homogenized in RIPA buffer (9806S, Cell Signaling Technologies, supplemented with 1% SDS and Protease/Phosphatase inhibitor, A32961, Invitrogen,) with sonication. Protein concentration was measured in clarified homogenates using a BCA protein assay (Thermo Fisher Scientific). Thirty micrograms of protein were loaded and separated in 4–12% gradient gels, and separated proteins were transferred to a nitrocellulose membrane. Membranes were blocked in 5% milk and incubated overnight in primary YAP antibody (sc-101199, 1:200, Santa Cruz Biotechnology). C2C12 cells were expanded under standard culture conditions in DMEM with 20% fetal bovine serum. For antibody validation experiments, C2C12 cells were seeded at a density of 5×10^4 cells/well in a six-well plate. After 24 h, cells were transiently transfected using the Jetprime transfection reagent (Polyplus) with either siRNA targeting YAP (SMARTpool ON-TARGETplus YAP1, Dharmacon) or scrambled control siRNA (ON-TARGETplus Non-targeting Control siRNA no. 1, Dharmacon) as described previously (19). Cells were homogenized 48 h posttransfection in RIPA buffer with sonication. In addition, we also used liver and lung homogenates of WT mice where YAP expression is known to be high. For all Western blots, membranes were also blocked in 3% BSA and incubated in primary phospho-YAP antibody (4911S, 1:300

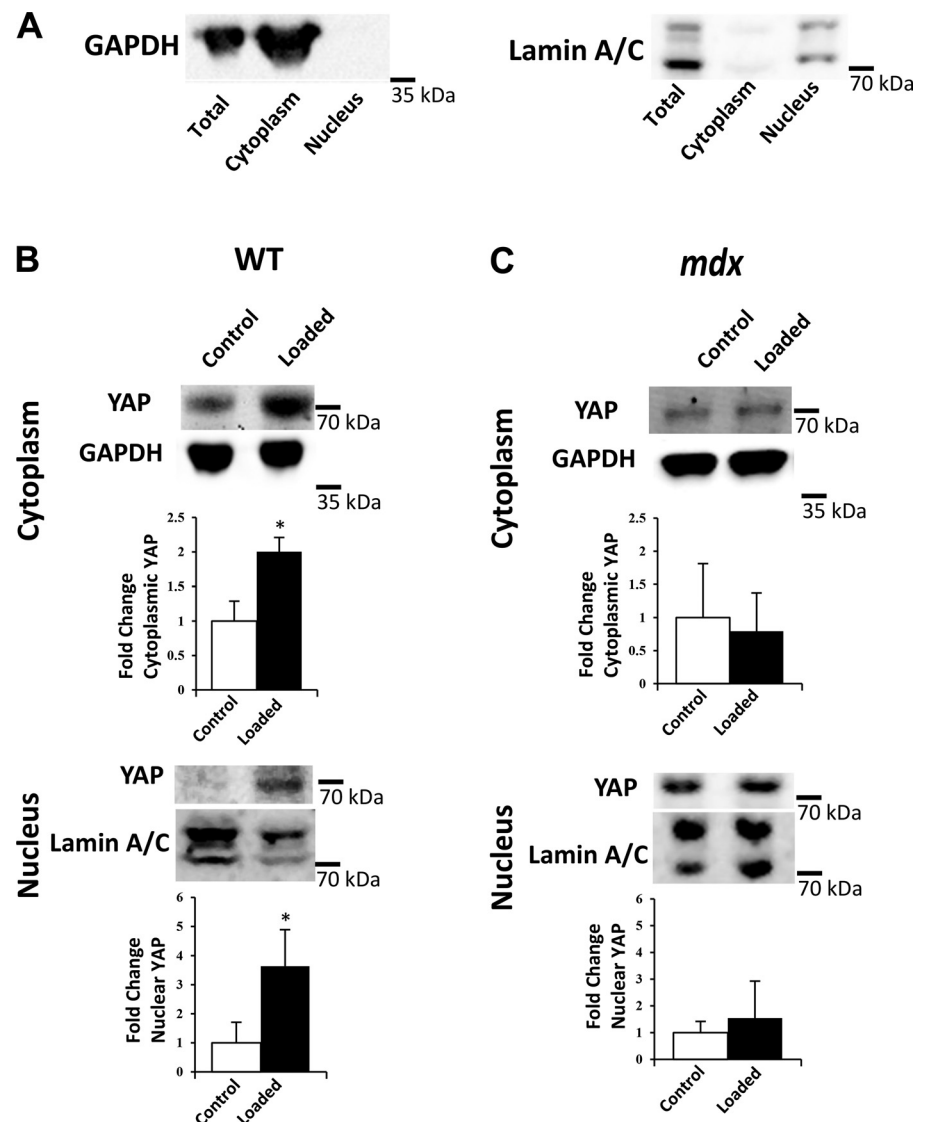


Fig. 2. Increased nuclear YAP with repeated isometric contractions in vivo is dependent on dystrophin. *A*: muscle homogenates were fractionated into nuclear and cytoplasmic components. Confirmation of effective nuclear/cytoplasmic fractionation was confirmed with absence of GAPDH expression in nuclear fraction, and absence of lamin A/C expression in cytoplasmic fraction. *B* and *C*: representative Western blots showing fold-change in cytoplasmic and nuclear YAP protein expression in WT and *mdx* muscles with or without isometric loading, relative to the unloaded conditions. The cropped blot in each panel is from a single gel and single exposure of 2 contiguous lanes. Densitometry measures were normalized to GAPDH and lamin A/C for cytoplasmic and nuclear fractions, respectively. Values are means \pm SD for TA muscles from 3 animals/genotype and loading condition. Although both nuclear and cytoplasmic YAP increase significantly in WT muscles after loading, no change is observed in *mdx* muscles after loading (* $P < 0.05$). A *t*-test was performed to determine statistical differences between control (no-load) and loaded conditions for WT and *mdx* muscles.

dilution, Cell Signaling Technology). Membranes were visualized after incubation with horseradish peroxidase-conjugated rabbit and mouse antibodies and ECL substrate (Thermo Fisher Scientific). Ponceau S staining was performed to ensure proper loading and to monitor the quality of protein transfer to the membrane. Bands were quantified using ImageJ software (National Institutes of Health) and normalized to GAPDH (6C5, 1:1,000, Santa Cruz Biotechnology). YAP and phospho-YAP expression were normalized to levels in control WT samples for obtaining the fold-change in expression for different groups.

Additional animals were used for *in vivo* experiments, and fractionation of the nuclear and cytoplasmic compartments was performed on isometrically loaded and contralateral WT and *mdx* TA muscles ($n = 3$ animals/group) according to previously developed techniques (9). Protein concentration was measured using a BCA protein assay (Thermo Fisher Scientific). In a 4–12% gradient gel, 20 μg of protein (cytosolic fraction) and up to 80 μg of protein (nuclear fraction) were loaded, and separated proteins were transferred to a nitrocellulose membrane. Membranes were blocked in 5% milk and incubated overnight in primary YAP antibody at 1: 200 dilution, GAPDH (6C5, 1:1,000, Santa Cruz Biotechnology) or lamin A/C (2032, 1:1,000, Cell Signaling). Membranes were visualized after incubation with horseradish peroxidase-conjugated rabbit and mouse antibodies and ECL substrate (Thermo Fisher Scientific). Bands were quantified using ImageJ software and normalized to GAPDH or lamin A/C for cytoplasmic and nuclear components, respectively.

In addition, Western blotting was performed using 30 μg of protein from whole muscle clarified homogenates of WT and *mdx* TA mus-

cles ($n = 3$ for WT and $n = 3$ for *mdx*), with membranes incubated overnight in primary paxillin antibody (610051, 1:5,000, BD Biosciences) and visualized as described above. Bands were quantified using ImageJ software and normalized to GAPDH. Paxillin expression was normalized to levels in WT samples for obtaining the fold-change in expression.

Immunofluorescence labeling and imaging. Isometrically loaded and contralateral WT and *mdx* TA muscles were sectioned (>3 sections/muscle) in the mid-belly at a thickness of 10 μm and fixed with 4% paraformaldehyde. Muscle sections were permeabilized with 0.5% Triton X-100-PBS, blocked in 3% BSA-PBS, and then labeled overnight with antibodies to YAP (sc-101199, 1:200, Santa Cruz Biotechnology). Sections were washed and labeled with secondary antibody Alexa Fluor 488 (1:100, Thermo Fisher Scientific). Sections were labeled in parallel and were mounted in Vectashield (Vector Laboratories, Burlingame, CA) with 4',6-diamidino-2-phenylindole (DAPI) added to label nuclei. Digital images of YAP and DAPI labeling were obtained with a Nikon Eclipse 50i microscope ($\times 20$ objective). Muscle sections were also labeled overnight with antibodies to paxillin (610051, 1:250) and secondary antibody Alexa Fluor 488 (1:100, Thermo Fisher Scientific) as described above. Digital images of paxillin labeling on muscle sections were obtained with a Zeiss LSM Duo ($\times 63$ objective) with the pinhole set at 1.0 Airy unit (z -section thickness = 1.0 μm , 3.6 pixels/ μm).

Quantitative real-time-PCR. For real-time (RT)-PCR detection of downstream YAP target transcripts, WT and *mdx* TA muscles ($n = 4$ each) were snap frozen and then homogenized in TRIzol reagent (Invitrogen, Carlsbad, CA). Total RNA was extracted according to the

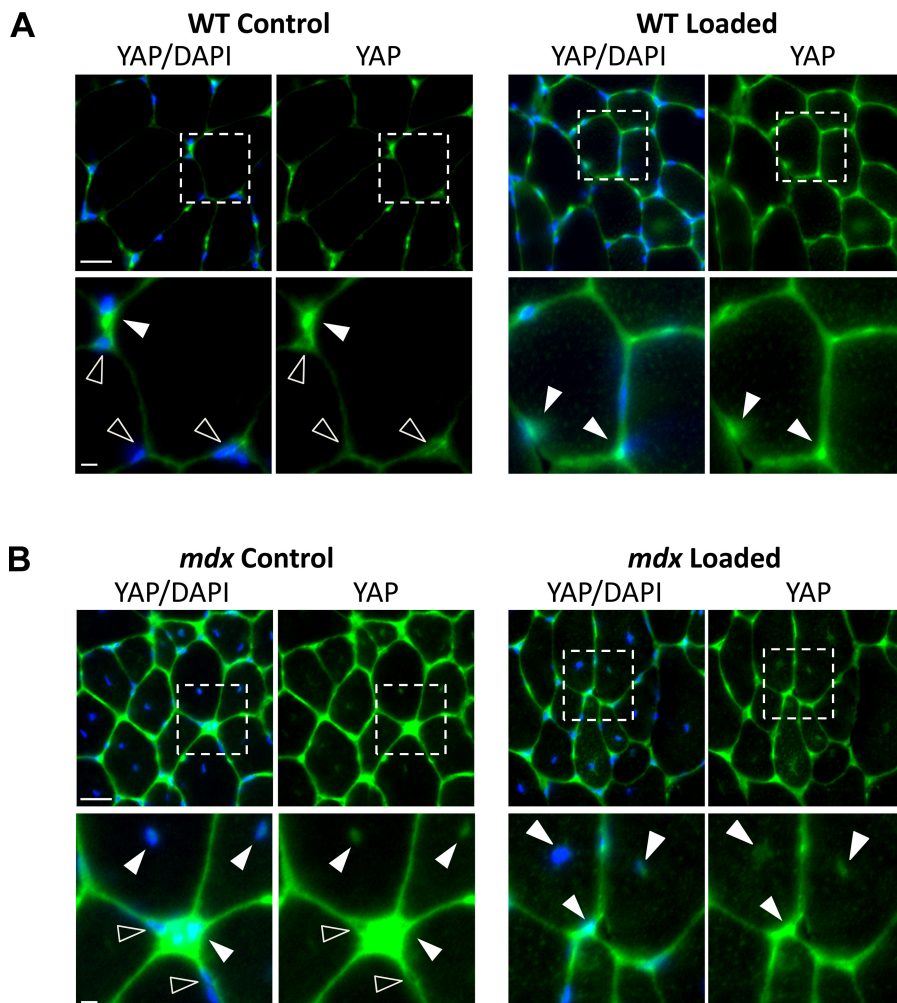


Fig. 3. YAP distribution in muscles in response to repeated maximal contractions *in vivo*. Representative cross sections showing YAP labeling (green) and nuclei (blue, DAPI). *Bottom* panels show magnification of area indicated by dotted white box in corresponding *top* panel. *A*: YAP labeling was increased in WT muscles with loading. *B*: control *mdx* muscles had increased YAP labeling compared with control WT muscles. However, no discernible increase was observed in *mdx* muscles with loading. Filled arrowheads indicate increased YAP nuclear occupancy, which includes central nuclei in both control and loaded *mdx* muscles. Open arrowheads indicate nuclei with less YAP occupancy. Scale bar = 25 μm . Magnified image, scale bar = 5 μm . Exposure time, brightness, and other fluorescent microscopy parameters were fixed and not altered between genotypes throughout experiments.

manufacturer's instructions and reverse transcribed. Quantitative RT-PCR was performed as described previously, with the ABI 7300 Sequence Detection System (Applied Biosystems, Foster City, CA) using SYBR green (43). Relative expression was determined by comparison to housekeeping gene *Gapdh* using geNorm software (v3.5, Ghent University Hospital, Ghent, Belgium). Transcripts for *Ankrd1*, *Vim*, *Ctgf*, and *Yap* were assessed. The primer sets used for PCR amplification are *Ankrd1* forward (F): GTCAAGAACTGT-GCTGGGAAGA, reverse (R): GTTCCACTGCCAGTGCAA; *Vim* F: AGATGGCTCGTCACCTTCGT, R: TCAATGTCCAGGGC-CATCTT; *Ctgf* F: AAAGTGCATCCGGACACCTAA, R: TGCAGC-CAGAAAGCTCAAACCT; *Yap* F: GGAAGGAGATGCAATGAA-CATAGA, R: CGTCCAAGATTTCCGAACTCA; and *Gapdh* F: CGTGTTCCTACCCCAATGT, R: TGTCATCATACTTGGCAG-GTTTCT.

Myofiber isolation and substrate stiffness. After mice were euthanized, the flexor digitorum brevis (FDB) muscles were harvested. To obtain single myofibers, muscles were placed into DMEM with 1% BSA, 50 μ g/ml gentamicin, and 4 mg/ml type I collagenase (C0130, Sigma) for 1–3 h at 37°C as previously described (17, 35). Myofibers were plated on extracellular matrix (ECM; Sigma E1270)-coated imaging dishes (P34G-1.0, 0–14-C, Matek) or ECM-coated dishes with soft (1 kPa) or stiff (50 kPa) hydrogels bound to glass bottom dishes (Softview, Easy coat hydrogels, Matrigen) overnight before fixation.

Myofibers on soft and stiff substrates were fixed with 4% paraformaldehyde. Myofibers were labeled with anti-YAP antibodies (1:200) with secondary antibody Alexa Fluor 568 (1:100, Thermo Fisher Scientific) as described above. Fibers were labeled in parallel and were mounted in Vectashield (Vector Laboratories) with DAPI added to label nuclei. Digital images of YAP and DAPI labeling were obtained with a Zeiss LSM Duo microscope ($\times 40$ objective) with the pinhole set at 1.5 Airy units (z -section thickness = 1.5 μ m, 2.28 pixels/ μ m). WT and *mdx* fibers were imaged, and z -stacked images were analyzed using ImageJ software. Average intensity of YAP nuclear localization was determined by measuring average intensity in the nucleus outlined by DAPI labeling. The procedures in image analysis (such as background removal and intensity measurement) were identical for each fiber/nucleus, precluding methodological bias by the experimenter. Each fiber/nucleus was processed in the same manner using identical algorithms (unbiased function of ImageJ to remove background, quantified region of interest) to obtain quantified measures from image analysis. Laser power, pinhole diameter, brightness and other confocal microscopy parameters were fixed and not altered between genotypes throughout experiments.

Statistical analysis. Statistical analyses were performed using SigmaStat 3.5 (San Rafael, CA). Data are presented as mean \pm SD unless otherwise noted. Statistical significance was assessed using one-way ANOVA for multiple groups when assumptions of normality and equal variance were met, one-way ANOVA on ranks for multiple groups when assumptions of normality and equal variance were not met, with post hoc analysis performed using the Student-Newman-Keuls method, and Student's *t*-test for comparisons between only two groups when assumptions of normality and equal variance were met or a Mann-Whitney rank-sum test for comparisons between only two groups when assumption of normality and equal variance were not met, with $P < 0.05$.

RESULTS

YAP is responsive to contractile loading only in healthy WT muscle. We used repeated maximal isometric contractions to the tibialis anterior (TA) muscle over a 2-h period for mechanical loading in vivo (Fig. 1A). The opposite TA muscles (unloaded) served as controls. We analyzed whole muscle homogenates from these in vivo loading experiments for total

YAP and phospho-YAP (the inactive, cytoplasmic form of YAP) expression (Fig. 1B). The phospho/total YAP ratio was significantly lower in WT-loaded muscles compared with control WT (unloaded) muscles (Fig. 1C). In *mdx* muscles, the phospho/total YAP ratio was decreased relative to the control WT muscles (Fig. 1C). In contrast to WT muscles, loading did not further decrease the phospho/total YAP ratio, suggesting a more active YAP signaling in the absence of dystrophin. In WT muscles, total YAP expression was increased with loading, whereas phospho-YAP expression was not altered with loading. Total YAP was increased in *mdx* muscle relative to the control WT muscles. Similarly, in *mdx* muscles total YAP regardless of loading was significantly more than in control

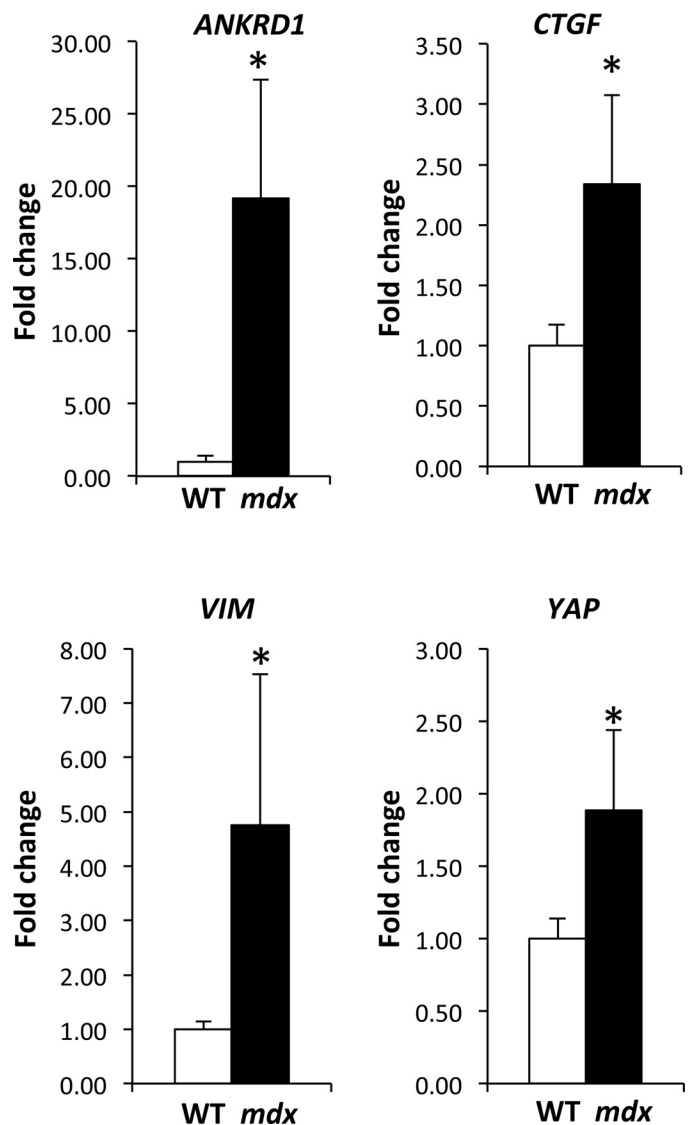


Fig. 4. YAP and YAP downstream targets are elevated in the absence of dystrophin. Fold-change for gene expression of transcripts for *Yap* and *Ankrd1*, *Vim*, and *Ctgf*, downstream targets of YAP. Values are normalized to housekeeping gene *GAPDH*. Values are means \pm SD for TA muscles from 4 animals/genotype. The high expression of *Ankrd1*, *Vim*, and *Ctgf* in *mdx* muscles, compared with WT muscles, is consistent with the elevated levels of active, nonphosphorylated YAP present in *mdx* muscles. A Mann-Whitney rank-sum test (*Vim*, *Ctgf*, *Ankrd1*) and *t*-test (*Yap*) were performed to determine statistical differences between WT and *mdx* muscles. * $P < 0.05$ from control, WT muscles.

WT muscles, suggesting a more active YAP signaling in the absence of dystrophin. In *mdx* muscle, the absence of dystrophin significantly lowered phospho-YAP expression regardless of loading.

We confirmed the specificity in skeletal muscle of the YAP antibody through the use of siRNA-mediated knockdown of YAP in C2C12 cells (Fig. 1D). In addition, we also used liver and lung homogenates (Fig. 1D), where YAP expression is known to be high, along with WT and *mdx* muscle homogenates (see supplemental data in Ref. 11 for additional validation of antibody specificity). We confirmed the specificity of the phospho-YAP antibody using Jurkat cells treated with calyculin A or LY294002 (9273, Cell Signaling Technologies), in addition to WT and *mdx* muscle homogenates (Fig. 1E). Calyculin A is a strong phosphatase inhibitor, while LY294002 is an inhibitor of phosphatidylinositol 3-kinase, with cells treated with LY294002 expressing low phospho-YAP expression (3) (see Ref. 38 for additional validation of antibody specificity).

To verify observations of nuclear signaling from whole muscle experiments in Fig. 1, both in WT and *mdx* muscle, we performed cell fractionation to confirm increased YAP localization to the nucleus occurs with mechanical loading in vivo (Fig. 2). Immediately following the completion of the isometric loading protocol (~2 h), muscles were fractionated to yield nuclear and cytoplasmic components, with fractionation confirmed by probing against GAPDH for cytosolic fraction and lamin A/C (Fig. 2A). In WT muscles, loading increases both cytoplasmic and nuclear YAP (Fig. 2B). However, in *mdx* muscles, loading does not change cytoplasmic or nuclear YAP, suggesting an impaired response to in vivo mechanical loading (Fig. 2C).

These findings were further verified with immunofluorescent labeling of total YAP on muscle tissue sections (Fig. 3), which indicated increased labeling of YAP with isometric loading in WT muscles (Fig. 3A), and with both conditions (unloaded and loaded) in *mdx* muscles (Fig. 3B). Consistent with our Western blot data, YAP occupancy of nuclei in WT muscles ($36.2 \pm 5.5\%$ nuclei, 393 nuclei analyzed) was markedly increased with loading ($74.7 \pm 9.1\%$ nuclei, 423

nuclei analyzed). In contrast, in *mdx* muscles most nuclei (~70%), including the central nuclei, were YAP positive, regardless of the loading condition ($71.4 \pm 7.3\%$, *mdx* unloaded nuclei, 560 nuclei analyzed; $71.9 \pm 7.2\%$ *mdx* loaded nuclei, 616 nuclei analyzed).

Downstream transcriptional targets of YAP are elevated in the absence of dystrophin. To confirm that the observed increased YAP nuclear translocation observed in unloaded *mdx* muscles was indicative of increased YAP activity in the nucleus, we examined the expression of several transcriptional targets of YAP. Relative expression of transcripts for *Yap* and three downstream YAP targets, *Ankrd1*, *Vim*, and *Ctgf* were determined using qRT-PCR. Gene expression of *Yap*, and the downstream targets, *Ankrd1*, *Vim*, and *Ctgf*, were significantly higher in *mdx* muscles compared with WT muscles (Fig. 4). These results further suggest a more “active” YAP signaling in *mdx*, in agreement with the reduced phospho/total Yap ratio in *mdx* muscles (Fig. 1).

Prior work has shown that cytoskeletal tension, or “pre-stress,” is an important modulator of muscle mechano-responsiveness (33, 47). The abundance of paxillin, a focal adhesion protein, is predictive of cytoskeletal tension, as it promotes the interaction of cytoskeleton with the extracellular matrix. Consistent with findings from others (47), we observed increased expression of paxillin in *mdx* muscles (Fig. 5) both by Western blotting (Fig. 5A) and by immunolabeling (Fig. 5B), suggesting that the *mdx* muscles are under increased cytoskeletal tension compared with WT muscles, potentially increasing mechano-responsiveness and contributing to the finding of constitutively active YAP.

Nuclear YAP is increased in plated muscle fibers in response to increased substrate stiffness. To test whether YAP signaling in *mdx* muscle could operate in a mechano-responsive nature under controlled in vitro conditions, we examined the YAP response of muscle fibers plated on substrates of different stiffness. Increased substrate stiffness can cause increased remodeling of the actin cytoskeleton in cells (13, 20, 48), and nuclear localization of YAP is responsive to substrate stiffness in a variety of cells (1, 10, 11, 30, 31, 49). Here, we used single isolated myofibers (Fig. 6A), plated on soft (1 kPa) or stiff (50

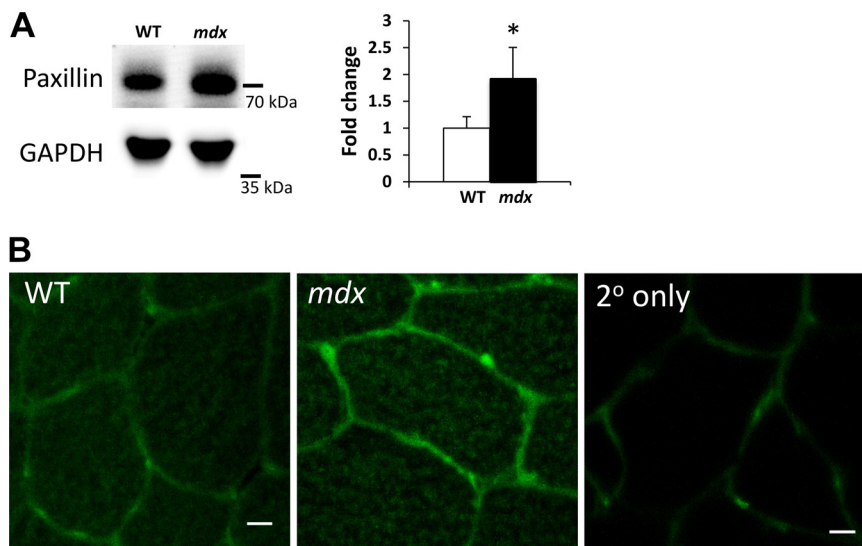


Fig. 5. The focal adhesion protein paxillin is increased in *mdx* muscles in vivo. Focal adhesions regulate force transfer between the myofiber cytoskeleton and its environment. **A**: Western blots of paxillin and GAPDH from WT and *mdx* muscles. The cropped blots in each panel are from a single gel and single exposure of 2 contiguous lanes. Densitometry measures were normalized to GAPDH expression and to WT muscles. **B**: representative confocal cross sections showing paxillin labeling (green) in WT and *mdx* muscle sections. Labeling with secondary antibody only shows a low background signal. These methods show that *mdx* muscles have increased paxillin expression and labeling compared with WT muscles. Values are means \pm SD for TA muscles from 3 animals/genotype. A *t*-test was performed on log-transformed data to determine statistical differences between groups. Scale bar = 10 μ m. **P* < 0.05 compared with WT.

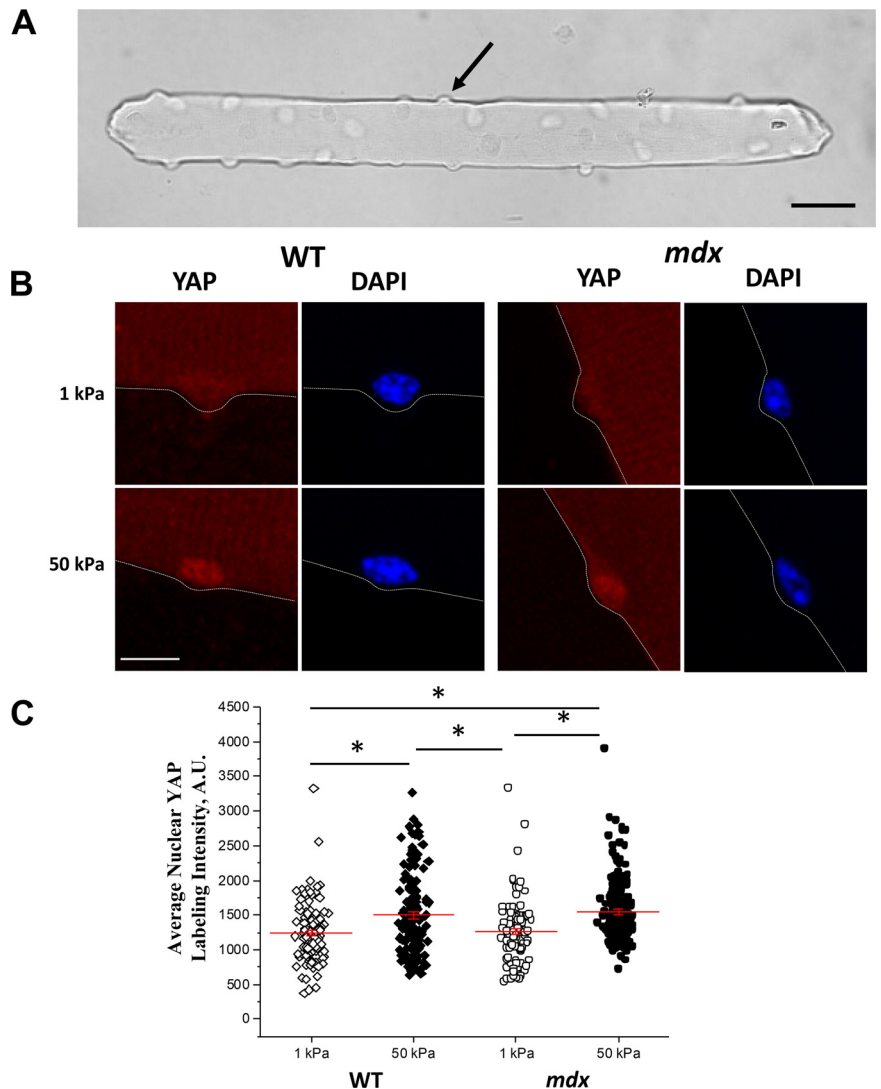


Fig. 6. YAP nuclear localization increases in response to a stiffer microenvironment. *A*: muscle fibers from the flexor digitorum brevis muscle were isolated and plated on soft or rigid substrates. Shown is an example of a typical single muscle fiber, which is an elongated multinucleated cell with peripherally located nuclei that are most easily visible along the edges (black arrow) when viewed *en face* in brightfield microscopy. Scale bar = 40 μm . *B*: healthy, WT muscle fibers and fibers from *mdx* mice (lacking dystrophin, a protein at the sarcolemma) were plated overnight on soft substrates (elastic modulus of gel = 1 kPa) and hard substrates (elastic modulus of gel = 50 kPa), and then labeled for YAP (red); nuclei were stained with DAPI (blue). *C*: nuclear localization of YAP was markedly increased in myofibers plated on a hard substrate. Scale bar = 10 μm . Scatter plots are from experiments repeated for ~ 100 nuclei assessed for each condition. The results indicate a significant difference in labeling intensity of YAP with a soft vs. a hard substrate ($*P < 0.05$). For all experiments, a one-way ANOVA on ranks was performed to determine statistical differences between groups.

kPa) levels of substrate stiffness. These commonly used in vitro conditions were used to determine the impact of dystrophin's absence on intrinsic YAP nuclear localization. Similar to other cell types, myofibers plated on the stiffer substrate showed a significant increase in nuclear YAP labeling intensity (Fig. 6*B*). In contrast to the in vivo results, muscle fibers lacking dystrophin had increased YAP nuclear localization with increasing substrate stiffness, similar to healthy WT controls in vitro (Fig. 6*C*). We posit that the YAP "off" condition (no labeling with soft substrate) is secondary to the artificially soft environment. This indicates that dystrophin deficiency does not impair the ability of YAP to translocate and suggests that the in vivo environment sets this hyperactivity of YAP in *mdx* muscle.

DISCUSSION

Transduction of mechanical force to cells through the extracellular matrix is important for tissue development, adaptation, and homeostasis. Frequently, tissue level control as a result of mechanical signals is due to the regulation of multiple genes by mechano-responsive factors (25). Here, we show for the first time that, in healthy skeletal muscle, nuclear YAP increases

significantly in response to in vivo muscle physiological loading and in mature, isolated muscle fibers to increases in in vitro substrate stiffness. Surprisingly, we found that *mdx* muscle exhibited elevated YAP activation, which was not further increased by muscle physiological loading. Our in vitro findings indicate that intrinsic YAP nuclear translocation is independent of dystrophin. Consistent with the notion that unloaded *mdx* muscle has more active YAP present, we observed significant increases in gene expression of *Yap*, and its downstream targets, *Ankrd1*, *Vim*, and *Ctgf* in *mdx* muscles compared with WT muscles. YAP, while considered a promoter of growth in various cell types, can lead to muscle degeneration and atrophy if constitutively active, due to cell type-specific differences in proliferative capacity (28).

The increased basal YAP signaling in *mdx* muscles, and lack of responsiveness of YAP signaling with loading relative to WT muscles, is likely not due to differences in active muscle force. We (46, 54) and others (8) have shown that absolute contractile force in *mdx* muscles is not lower than in WT muscles. The diminished response to loading could be due to the high levels of YAP already present in control (unloaded) *mdx* muscles. It is more likely that *mdx* muscles could be in a

“preloaded” state with more active YAP signaling, as *mdx* muscle have increased stiffness (2, 21, 32, 33) due to increased fibrosis (21) and increased expression of cytoskeleton components, such as microtubules (4, 32, 33, 42) and desmin (4, 42). Given the potential preactivated state of mechano-signaling in *mdx* muscle, it is not surprising that loading did not further enhance YAP signaling. The lack of responsiveness in YAP signaling to loading and increased basal YAP signaling could also be due to alterations in the nuclear envelope in *mdx* muscle (26) and altered cell population proportions in dystrophic muscles.

Despite missing a key protein in the sarcolemma, *mdx* muscle fibers appeared to be mechano-responsive when plated on substrates with varying stiffnesses. Cell spreading onto a substrate uses focal adhesions to stabilize the actin cytoskeleton to the cell membrane, and this involves YAP (41). Interestingly, deficiencies in dystrophin lead to upregulation of numerous focal adhesion proteins (47), including paxillin, presumably to compensate for the lack of dystrophin at the sarcolemma. It is likely that in vivo the dystrophic muscle is stiffer, driving the basal increase in YAP that cannot be further exacerbated by load. Changes in substrate stiffness induce changes in the cellular cytoskeleton, such as an increased remodeling of the entire actin cytoskeleton seen with increasing substrate stiffness (13, 20, 48). These variables could explain why YAP appears to be responsive in *mdx* myofibers in vitro, but unequivocally unresponsive to in vivo loading. Interestingly, targeting the cytoskeleton can reverse aspects of the dystrophic muscle phenotype (4, 32, 33, 42). It should be noted that the extreme changes in substrate stiffness used for in vitro assays likely do not occur with anatomically attached muscles tested in vivo.

Studies on YAP protein expression in *mdx* muscles have reported conflicting results. Consistent with our findings, one study reported increased total YAP and reduced phospho/total YAP (increased YAP signaling) compared with WT muscles (23, 52). Other studies on mineralocorticoid receptors and fibrosis in *mdx* muscles have reported increased gene and protein expression of *Ankrd1*, *Ctgf*, and *Vim* (7, 22, 39), with these genes being known downstream targets of YAP (50, 53). Previous studies have also shown that gene expression profiling of skeletal muscle from constitutively active YAP mutant mice is similar to *mdx* skeletal muscle mice (28). In contrast, another study found unchanged total YAP and increased phospho/total YAP (reduced YAP signaling) compared with WT dorsiflexor muscles (23, 52).

Recent data indicate that force can be transmitted directly to the nucleus, where force-transmitting structures also reside. YAP nuclear translocation occurs via changes in nuclear pores that occur with mechanical stress, with immediate nuclear export observed upon force release (12). This rapid response fits a recently described explanation of YAP nuclear import-export kinetics (12) and could also explain the apparent variability in findings from various papers of YAP nuclear signaling in skeletal muscle, as time before harvesting and freezing of muscles likely varies. Variability of YAP expression in different muscles could also contribute to the variability of findings (52). In addition, previously published reports have shown both a significant change and no change in the ratio of phosphorylated to total YAP after in vivo overloading of a muscle (hindlimb unloading-reloading and synergist ablation,

respectively) (6, 18). The acute nature of our experiments (240 repetitions of isometric loading) compared with the longer duration of both hindlimb unloading-reloading (up to 28 days) and synergist ablation experiments (up to 14 days) could impact YAP signaling in these tissues. In addition, the differences in the forces applied in these experiments could also contribute to the changes in YAP signaling observed.

In summary, there is growing evidence of YAP as a marker for nuclear mechanotransduction in many non-muscle cell types. We show, for the first time, similar findings for isolated mature muscle fibers exposed to increased substrate rigidity, as well as subsequent to in vivo loading via repeated maximal contractions. Although YAP signaling in isolated in vitro muscle fibers lacking dystrophin appears to be mechano-responsive, the constitutively active YAP signaling in *mdx* muscle in vivo, which is unresponsive to loading, is indicative of impaired nuclear mechanotransduction. This impaired mechano-responsiveness is possibly due to the aberrant increase in cytoskeletal and extracellular matrix stiffness. Future studies will look directly into the role of increased cytoskeletal elements, and pharmacological interventions to reduce cytoskeletal density, in addition to fibrosis, in reducing the hyperactive YAP signaling in *mdx* muscle. Aberrant mechano-signaling in *mdx* muscles with hyperactive YAP signaling is an important aspect of the underlying molecular basis of the pathology, which could underlie, or at least contribute to the pathogenesis of DMD.

ACKNOWLEDGMENTS

The data sets generated during and/or analyzed during the current study are available from the corresponding author on reasonable request.

GRANTS

This work was supported by grants from the National Institutes of Health, including training grant T32 AR-007592 and MDA development grant 577897 (S. R. Iyer), and research grants R01-AR059179 and R21-AR067872-01 (R. M. Lovering).

DISCLOSURES

No conflicts of interest, financial or otherwise, are declared by the authors.

AUTHOR CONTRIBUTIONS

S.R.I. and R.M.L. conceived and designed research; S.R.I., J.P.S., and R.M.L. performed experiments; S.R.I., J.P.S., E.E.S., E.S.F., and R.M.L. analyzed data; S.R.I., S.B.S., C.W.W., J.P.S., E.E.S., E.S.F., and R.M.L. interpreted results of experiments; S.R.I. and R.M.L. prepared figures; S.R.I., S.B.S., C.W.W., and R.M.L. drafted manuscript; S.R.I., S.B.S., C.W.W., J.P.S., E.E.S., E.S.F., and R.M.L. edited and revised manuscript; S.R.I., S.B.S., C.W.W., J.P.S., E.E.S., E.S.F., and R.M.L. approved final version of manuscript.

REFERENCES

1. Aragona M, Panciera T, Manfrin A, Giulitti S, Michielin F, Elvassore N, Dupont S, Piccolo S. A mechanical checkpoint controls multicellular growth through YAP/TAZ regulation by actin-processing factors. *Cell* 154: 1047–1059, 2013. doi:10.1016/j.cell.2013.07.042.
2. Baltgalvis KA, Jaeger MA, Fitzsimons DP, Thayer SA, Lowe DA, Ervasti JM. Transgenic overexpression of γ -cytoplasmic actin protects against eccentric contraction-induced force loss in *mdx* mice. *Skeletal Muscle* 1: 32, 2011. doi:10.1186/2044-5040-1-32.
3. Basu S, Totty NF, Irwin MS, Sudol M, Downward J. Akt phosphorylates the Yes-associated protein, YAP, to induce interaction with 14-3-3 and attenuation of p73-mediated apoptosis. *Mol Cell* 11: 11–23, 2003. doi:10.1016/S1097-2765(02)00776-1.

4. Belanto JJ, Olthoff JT, Mader TL, Chamberlain CM, Nelson DM, McCourt PM, Talsness DM, Gundersen GG, Lowe DA, Ervasti JM. Independent variability of microtubule perturbations associated with dystrophinopathy. *Hum Mol Genet* 25: 4951–4961, 2016. doi:10.1093/hmg/ddw318.
5. Bertrand AT, Ziaei S, Ehret C, Duchemin H, Mamchaoui K, Bigot A, Mayer M, Quijano-Roy S, Desguerre I, Lainé J, Ben Yaou R, Bonne G, Coirault C. Cellular microenvironments reveal defective mechanosensing responses and elevated YAP signaling in LMNA-mutated muscle precursors. *J Cell Sci* 127: 2873–2884, 2014. doi:10.1242/jcs.144907.
6. Brooks MJ, Hajira A, Mohamed JS, Alway SE. Voluntary wheel running increases satellite cell abundance and improves recovery from disuse in gastrocnemius muscles from mice. *J Appl Physiol* 124: 1616–1628, 2018. doi:10.1152/jappphysiol.00451.2017.
7. Chadwick JA, Hauck JS, Lowe J, Shaw JJ, Guttridge DC, Gomez-Sanchez CE, Gomez-Sanchez EP, Rafael-Fortney JA. Mineralocorticoid receptors are present in skeletal muscle and represent a potential therapeutic target. *FASEB J* 29: 4544–4554, 2015. doi:10.1096/fj.15-276782.
8. Dellorusso C, Crawford RW, Chamberlain JS, Brooks SV. Tibialis anterior muscles in mdx mice are highly susceptible to contraction-induced injury. *J Muscle Res Cell Motil* 22: 467–475, 2001. doi:10.1023/A:1014587918367.
9. Dimauro I, Pearson T, Caporossi D, Jackson MJ. A simple protocol for the subcellular fractionation of skeletal muscle cells and tissue. *BMC Res Notes* 5: 513, 2012. doi:10.1186/1756-0500-5-513.
10. Driscoll TP, Cosgrove BD, Heo SJ, Shurden ZE, Mauck RL. Cytoskeletal to nuclear strain transfer regulates YAP signaling in mesenchymal stem cells. *Biophys J* 108: 2783–2793, 2015. doi:10.1016/j.bpj.2015.05.010.
11. Dupont S, Morsut L, Aragona M, Enzo E, Giulitti S, Cordenonsi M, Zanconato F, Le Digabel J, Forcato M, Bicciato S, Elvassore N, Piccolo S. Role of YAP/TAZ in mechanotransduction. *Nature* 474: 179–183, 2011. doi:10.1038/nature10137.
12. Elosegui-Artola A, Andreu I, Beedle AEM, Lezamiz A, Uroz M, Kosmalska AJ, Oriá R, Kechagia JZ, Rico-Lastres P, Le Roux AL, Shanahan CM, Trepát X, Navajas D, Garcia-Manes S, Roca-Cusachs P. Force triggers YAP nuclear entry by regulating transport across nuclear pores. *Cell* 171: 1397–1410.e14, 2017. doi:10.1016/j.cell.2017.10.008.
13. Engler A, Bacakova L, Newman C, Hategan A, Griffin M, Discher D. Substrate compliance versus ligand density in cell on gel responses. *Biophys J* 86: 617–628, 2004. doi:10.1016/S0006-3495(04)74140-5.
14. Fischer M, Rikeit P, Knaus P, Coirault C. YAP-mediated mechanotransduction in skeletal muscle. *Front Physiol* 7: 41, 2016. doi:10.3389/fphys.2016.00041.
15. Gabriel BM, Hamilton DL, Tremblay AM, Wackerhage H. The Hippo signal transduction network for exercise physiologists. *J Appl Physiol* (1985) 120: 1105–1117, 2016. doi:10.1152/jappphysiol.01076.2015.
16. Gnimassou O, Francaux M, Deldicque L. Hippo pathway and skeletal muscle mass regulation in mammals: a controversial relationship. *Front Physiol* 8: 190, 2017. doi:10.3389/fphys.2017.00190.
17. Goodall MH, Ward CW, Pratt SJP, Bloch RJ, Lovering RM. Structural and functional evaluation of branched myofibers lacking intermediate filaments. *Am J Physiol Cell Physiol* 303: C224–C232, 2012. doi:10.1152/ajpcell.00136.2012.
18. Goodman CA, Dietz JM, Jacobs BL, McNally RM, You JS, Hornberger TA. Yes-associated protein is up-regulated by mechanical overload and is sufficient to induce skeletal muscle hypertrophy. *FEBS Lett* 589: 1491–1497, 2015. doi:10.1016/j.febslet.2015.04.047.
19. Gupta A, Anderson H, Buo AM, Moorner MC, Ren M, Stains JP. Communication of cAMP by connexin43 gap junctions regulates osteoblast signaling and gene expression. *Cell Signal* 28: 1048–1057, 2016. doi:10.1016/j.cellsig.2016.04.014.
20. Gupta M, Sarangi BR, Deschamps J, Nematbakhsh Y, Callan-Jones A, Margadant F, Mège RM, Lim CT, Voituriez R, Ladoux B. Adaptive rheology and ordering of cell cytoskeleton govern matrix rigidity sensing. *Nat Commun* 6: 7525, 2015. doi:10.1038/ncomms8525.
21. Hakim CH, Grange RW, Duan D. The passive mechanical properties of the extensor digitorum longus muscle are compromised in 2- to 20-month-old mdx mice. *J Appl Physiol* (1985) 110: 1656–1663, 2011. doi:10.1152/jappphysiol.01425.2010.
22. Holland A, Henry M, Meleady P, Winkler CK, Krautwald M, Brinkmeier H, Ohlendeck K. Comparative label-free mass spectrometric analysis of mildly versus severely affected mdx mouse skeletal muscles identifies annexin, lamin, and vimentin as universal dystrophic markers. *Molecules* 20: 11317–11344, 2015. doi:10.3390/molecules200611317.
23. Hulmi JJ, Oliveira BM, Silvennoinen M, Hoogaars WM, Ma H, Pierre P, Pasternack A, Kainulainen H, Ritvos O. Muscle protein synthesis, mTORC1/MAPK/Hippo signaling, and capillary density are altered by blocking of myostatin and activins. *Am J Physiol Endocrinol Metab* 304: E41–E50, 2013. doi:10.1152/ajpendo.00389.2012.
24. Huraskin D, Eiber N, Reichel M, Zidek LM, Kravic B, Bernkopf D, von Maltzahn J, Behrens J, Hashemolhosseini S. Wnt/ β -catenin signaling via Axin2 is required for myogenesis and, together with YAP/Taz and Tead1, active in Ila/IIx muscle fibers. *Development* 143: 3128–3142, 2016. doi:10.1242/dev.139907.
25. Isermann P, Lammerding J. Nuclear mechanics and mechanotransduction in health and disease. *Curr Biol* 23: R1113–R1121, 2013. doi:10.1016/j.cub.2013.11.009.
26. Iyer SR, Shah SB, Valencia AP, Schneider MF, Hernández-Ochoa EO, Stains JP, Blemker SS, Lovering RM. Altered nuclear dynamics in MDX myofibers. *J Appl Physiol* (1985) 122: 470–481, 2017. doi:10.1152/jappphysiol.00857.2016.
27. Iyer SR, Valencia AP, Hernández-Ochoa EO, Lovering RM. In vivo assessment of muscle contractility in animal studies. *Methods Mol Biol* 1460: 293–307, 2016. doi:10.1007/978-1-4939-3810-0_20.
28. Judson RN, Gray SR, Walker C, Carroll AM, Itzstein C, Lionikas A, Zammit PS, De Bari C, Wackerhage H. Constitutive expression of Yes-associated protein (Yap) in adult skeletal muscle fibres induces muscle atrophy and myopathy. *PLoS One* 8: e59622, 2013. doi:10.1371/journal.pone.0059622.
29. Judson RN, Tremblay AM, Knopp P, White RB, Urcia R, De Bari C, Zammit PS, Camargo FD, Wackerhage H. The Hippo pathway member Yap plays a key role in influencing fate decisions in muscle satellite cells. *J Cell Sci* 125: 6009–6019, 2012. doi:10.1242/jcs.109546.
30. Kaneko K, Ito M, Naoe Y, Lacy-Hulbert A, Ikeda K. Integrin α v in the mechanical response of osteoblast lineage cells. *Biochem Biophys Res Commun* 447: 352–357, 2014. doi:10.1016/j.bbrc.2014.04.006.
31. Kegelman CD, Mason DE, Dawahare JH, Horan DJ, Vigil GD, Howard SS, Robling AG, Bellido TM, Boerckel JD. Skeletal cell YAP and TAZ combinatorially promote bone development. *FASEB J* 32: 2706–2721, 2018. doi:10.1096/fj.201700872R.
32. Kerr JP, Robison P, Shi G, Bogush AI, Kempema AM, Hexum JK, Becerra N, Harki DA, Martin SS, Raiteri R, Prosser BL, Ward CW. Detyrosinated microtubules modulate mechanotransduction in heart and skeletal muscle. *Nat Commun* 6: 8526, 2015. doi:10.1038/ncomms9526.
33. Khairallah RJ, Shi G, Sbrana F, Prosser BL, Borroto C, Mazaitis MJ, Hoffman EP, Mahurkar A, Sachs F, Sun Y, Chen YW, Raiteri R, Lederer WJ, Dorsey SG, Ward CW. Microtubules underlie dysfunction in duchenne muscular dystrophy. *Sci Signal* 5: ra56, 2012. doi:10.1126/scisignal.2002829.
34. Lovering RM, De Deyne PG. Contractile function, sarcolemma integrity, and the loss of dystrophin after skeletal muscle eccentric contraction-induced injury. *Am J Physiol Cell Physiol* 286: C230–C238, 2004. doi:10.1152/ajpcell.00199.2003.
- 34a. Lovering RM, Hakim M, Moorman CT III, De Deyne PG. The contribution of contractile pre-activation to loss of function after a single lengthening contraction. *J Biomech* 38: 1501–1507, 2005. doi:10.1016/j.jbiomech.2004.07.008.
35. Lovering RM, Michaelson L, Ward CW. Malformed mdx myofibers have normal cytoskeletal architecture yet altered EC coupling and stress-induced Ca^{2+} signaling. *Am J Physiol Cell Physiol* 297: C571–C580, 2009. doi:10.1152/ajpcell.00087.2009.
36. Lovering RM, Porter NC, Bloch RJ. The muscular dystrophies: from genes to therapies. *Phys Ther* 85: 1372–1388, 2005.
37. Lovering RM, Roche JA, Goodall MH, Clark BB, McMillan A. An in vivo rodent model of contraction-induced injury and non-invasive monitoring of recovery. *J Vis Exp* (51): 2782, 2011. doi:10.3791/2782.
38. Lu L, Finegold MJ, Johnson RL. Hippo pathway coactivators Yap and Taz are required to coordinate mammalian liver regeneration. *Exp Mol Med* 50: e423, 2018. doi:10.1038/emmm.2017.205.
39. Morales MG, Gutierrez J, Cabello-Verrugio C, Cabrera D, Lipson KE, Goldschmeding R, Brandan E. Reducing CTGF/CCN2 slows down mdx muscle dystrophy and improves cell therapy. *Hum Mol Genet* 22: 4938–4951, 2013. doi:10.1093/hmg/ddt352.
40. Morikawa Y, Zhang M, Heallen T, Leach J, Tao G, Xiao Y, Bai Y, Li W, Willerson JT, Martin JF. Actin cytoskeletal remodeling with pro-

- trusion formation is essential for heart regeneration in Hippo-deficient mice. *Sci Signal* 8: ra41, 2015. doi:10.1126/scisignal.2005781.
41. Nardone G, Oliver-De La Cruz J, Vrbsky J, Martini C, Pribyl J, Skladal P, Peřl M, Caluori G, Pagliari S, Martino F, Maceckova Z, Hajduch M, Sanz-Garcia A, Pugno NM, Stokin GB, Forte G. YAP regulates cell mechanics by controlling focal adhesion assembly. *Nat Commun* 8: 15321, 2017. doi:10.1038/ncomms15321.
 42. Nelson DM, Lindsay A, Judge LM, Duan D, Chamberlain JS, Lowe DA, Ervasti JM. Variable rescue of microtubule and physiological phenotypes in mdx muscle expressing different miniaturized dystrophins. *Hum Mol Genet* 27: 2090–2100, 2018. doi:10.1093/hmg/ddy113.
 43. Niger C, Howell FD, Stains JP. Interleukin-1 β increases gap junctional communication among synovial fibroblasts via the extracellular-signal-regulated kinase pathway. *Biol Cell* 102: 37–49, 2012. doi:10.1042/BC20090056.
 44. Panciera T, Azzolin L, Cordenonsi M, Piccolo S. Mechanobiology of YAP and TAZ in physiology and disease. *Nat Rev Mol Cell Biol* 18: 758–770, 2017. doi:10.1038/nrm.2017.87.
 45. Pratt SJP, Shah SB, Ward CW, Inacio MP, Stains JP, Lovering RM. Effects of in vivo injury on the neuromuscular junction in healthy and dystrophic muscles. *J Physiol* 591: 559–570, 2013. doi:10.1113/jphysiol.2012.241679.
 46. Pratt SJ, Shah SB, Ward CW, Kerr JP, Stains JP, Lovering RM. Recovery of altered neuromuscular junction morphology and muscle function in mdx mice after injury. *Cell Mol Life Sci* 72: 153–164, 2015. doi:10.1007/s00018-014-1663-7.
 47. Sen S, Tewari M, Zajac A, Barton E, Sweeney HL, Discher DE. Upregulation of paxillin and focal adhesion signaling follows Dystroglycan Complex deletions and promotes a hypertensive state of differentiation. *Eur J Cell Biol* 90: 249–260, 2011. doi:10.1016/j.ejcb.2010.06.005.
 48. Solon J, Levental I, Sengupta K, Georges PC, Janmey PA. Fibroblast adaptation and stiffness matching to soft elastic substrates. *Biophys J* 93: 4453–4461, 2007. doi:10.1529/biophysj.106.101386.
 49. Stearns-Reider KM, D'Amore A, Beezhold K, Rothrauff B, Cavalli L, Wagner WR, Vorp DA, Tsamis A, Shinde S, Zhang C, Barchowsky A, Rando TA, Tuan RS, Ambrosio F. Aging of the skeletal muscle extracellular matrix drives a stem cell fibrogenic conversion. *Aging Cell* 16: 518–528, 2017. doi:10.1111/ace1.12578.
 50. Thongon N, Castiglioni I, Zucal C, Latorre E, D'Agostino V, Bauer I, Pancher M, Ballestrero A, Feldmann G, Nencioni A, Provenzani A. The GSK3 β inhibitor BIS I reverts YAP-dependent EMT signature in PDAC cell lines by decreasing SMADs expression level. *Oncotarget* 7: 26551–26566, 2016. doi:10.18632/oncotarget.8437.
 51. Udan RS, Kango-Singh M, Nolo R, Tao C, Halder G. Hippo promotes proliferation arrest and apoptosis in the Salvador/Warts pathway. *Nat Cell Biol* 5: 914–920, 2003. doi:10.1038/ncb1050.
 52. Vita GL, Polito F, Oteri R, Arrigo R, Ciranni AM, Musumeci O, Messina S, Rodolico C, Di Giorgio RM, Vita G, Aguenouz M. Hippo signaling pathway is altered in Duchenne muscular dystrophy. *PLoS One* 13: e0205514, 2018. doi:10.1371/journal.pone.0205514.
 53. Watt KL, Turner BJ, Hagg A, Zhang X, Davey JR, Qian H, Beyer C, Winbanks CE, Harvey KF, Gregorevic P. The Hippo pathway effector YAP is a critical regulator of skeletal muscle fibre size. *Nat Commun* 6: 6048, 2015. doi:10.1038/ncomms7048.
 54. Xu S, Pratt SJP, Spangenburg EE, Lovering RM. Early metabolic changes measured by ¹H MRS in healthy and dystrophic muscle after injury. *J Appl Physiol (1985)* 113: 808–816, 2012. doi:10.1152/jappphysiol.00530.2012.
 55. Zhao K, Shen C, Lu Y, Huang Z, Li L, Rand CD, Pan J, Sun XD, Tan Z, Wang H, Xing G, Cao Y, Hu G, Zhou J, Xiong WC, Mei L. Muscle Yap is a regulator of neuromuscular junction formation and regeneration. *J Neurosci* 37: 3465–3477, 2017. doi:10.1523/JNEUROSCI.2934-16.2017.
 56. Zhu C, Li L, Zhao B. The regulation and function of YAP transcription co-activator. *Acta Biochim Biophys Sin (Shanghai)* 47: 16–28, 2015. doi:10.1093/abbs/gmu110.